Metrologia 16, 169–175 (1980)

metrologia

Automatic Recording Laser Interferometer for Line Standards up to 2 m

H. Matsumoto, S. Seino and Y. Sakurai[1]

National Research Laboratory of Metrology, 1-1-4 Umezono, Sakura-mura, Niihari-gun, Ibaraki 305, Japan

Received: November 15, 1979 and in revised form June 2, 1980

Abstract

A description is given of an automaic recording laser interferometer for calibrating line standards up to 2 m based on Eppenstein's principle, and various factors which limit the measuring accuracies are also investigated in detail. This fringe-counting interferometer uses two corner cube reflectors. One reflector is mounted with the objective of a photoelectric miscroscope on a carriage which moves at a uniform speed of 10 to 300 mm/min on an air track. An electric pulse, which corresponds to the center of a graduation line and is a gate signal for counting interference fringes, is produced by the zero crossing method from the derivative of a signal obtained when the graduation line image goes across a slit. The reflectors generate two different interference fringes in phase quadrature by using their polarization properties in reflection, so that fringe resolving power is raised to $\lambda/16$.

The experimental results on line standards show that the standard deviation of a graduation line positioning is 0.04 μm and the accuracy of measurement on a 1 m line-interval is 0.08 μm in standard deviation.

1. Introduction

Various kinds of interferometers for calibrating line standards in terms of wavelength of light have already been put to practical use [1, 2, 3, 4, 5, 6, 7]. A distinction can be drawn between an interferometer in which high accuracy of measurement is preferred rather than high efficiency of measurement (type A), and reversely, an interferometer in which high efficiency is preferred rather than high accuracy (type B). Type A is designed for calibrating line standards with the high accuracy required in national standards, while type B is designed for calibrating practical line standards and inspecting products in inspection facilities and production works.

A principal difference in function between both types of interferometers exists in movement of the photoelectric microscope. In type A, the photoelectric microscope stops at each graduation line, the graduation line is positioned, and interference fringes are read. While type B moves continuously at a certain speed and generates photoelectric line signals as it passes through the graduation lines, by which interference fringes are automatically counted and recorded.

Although the present interferometer belongs to type B, it is designed for measuring line standards with the highest efficiency and with the highest possible accuracy [8, 9, 10]. In this type of interferometer, any error of measurement is mainly caused by mispositioning of the graduation lines with the photoelectric microscope. Therefore, in the present interferometer, a sheet of teflon fluoracarbon resin is used on the sliding face of the photoelectric microscope carriage under suitable conditions, to reduce speed fluctuation of the carriage and to decrease errors caused by this speed fluctuation.

2. Principle of Measurement

2.1. Optical System

Figure 1 shows schematically the optical system of the interferometer. A light beam from the stabilized He-Ne laser SL is condensed in the center of the pinhole S1 by the lens L1 after passing through the polarizer P, and is collimated by the collimator lens L2. The pinhole serves to interrupt stray light beams only and is large enough to allow all condensed laser beams to pass through it. The reflector M1 is attached to a remote-controllable hinge. For measuring line standards, this reflector is placed outside the optical path, and for measuring the refractive index of air it is arranged in the position shown in Fig. 1 to guide the collimated beam to a refractometer. The refractometer, a Fizeau-type interferometer, consists of two 20%-transparent mirrors B3, B4 in which is inserted a vacuum cell V about 500 mm long. Interference fringes formed both by light beams passing in the air and in the vacuum are projected on an observation screen, and the phase difference between both fringes is measured by the reading device with a vernier scale.

In measuring the line standard S, the collimated beam is devided into two segments by the beam splitter

[1] Now at Chiba Institute of Technology, 17–I, Tsudanuma-2, Narashino, Chiba 275, Japan

0026-1394/80/0016/0169/$01.40

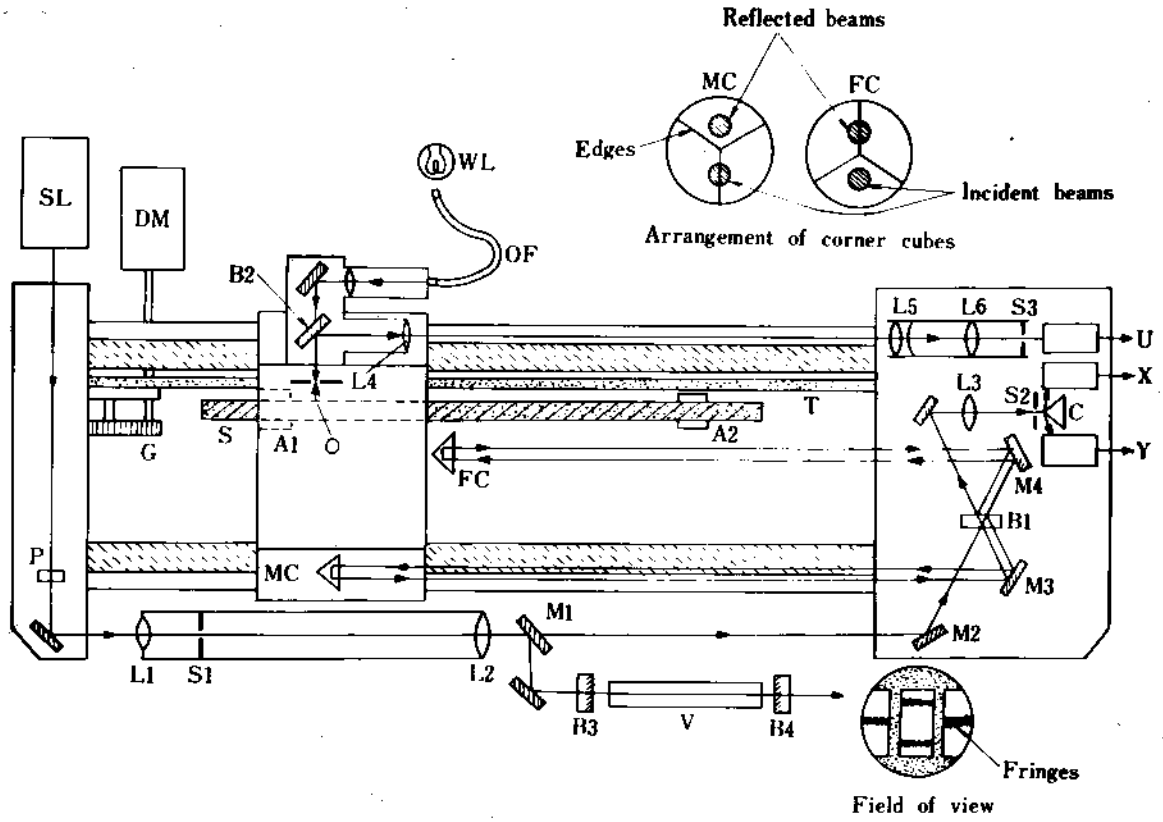

Fig. 1. Schematic diagram of the interferometer: SL, stabilized He-Ne laser; P, polarizer; M1 to M4, reflectors; L1 to L6, objective lenses; B1 to B4, beam splitters; MC, FC, corner cubes; C, prism; S1, S2, pinholes; S3, slit; OF, optical fiber; WL, white light source; S, line standard; A1, A2, adjusting tables; U, X, Y, photomultiplier tubes; DM, motor; G, gear; T, steel tape; V, vacuum chamber; O, graduation line

B1. One beam enters the fixed corner cube FC mounted on the rest supporting the line standard, and the other beam enters the moving corner cube MC mounted on the carriage. These corner cubes are so arranged that their edges are separated in directions by an angle of 60°. Namely, they overlap at the edges if one of them is rotated by that angle. The faces of the corner cubes are shown in Fig. 1. If the collimated beam enters so that its wavefront is divided symmetrically into two segments by the vertical edge in both corner cubes, these two segments are reflected symmetrically relative to the corner point of the cube respectively. The reflected beams from corner cubes FC and MC re-encounter the beam splitter B1 to form interference fringes. In such an arrangement, the light beam is divided into two beams of different phases by polarization properties of the corner cubes and the beam splitter [11]. Moreover, the plane of polarization for the incident beam should be set by rotating the polarization plate P at such an angle that the phase difference between these beams forms an angle of 90°.

The photoelectric microscope consists of two principal components. One component, including an illumination system for graduation lines, an objective L4, and a reflector B2, is mounted on the carriage. The other component, including a projection lens L5, an expansion lens L6, a slit S3, and a photoelectric detector U, is secured to a board as shown in Fig. 1 on the right.

The graduation lines are illuminated by light from a white light source WL provided outside the instrument through the optical fiber OF and the optical system (Köhler's illumination). Images of the graduation lines are first formed in full size at the position of the object point of the expansion lens L6 (numerical aperture 0.25) by the objective L4 (numerical aperture 0.12, focal length 210 mm) and the projection lens L5, and subsequently are formed at a magnification of ten on the slit S3. During measurement, the formed graduation line image moves on the surface of the slit S3 as the carriage travels linearly. Therefore, if the slit width is nearly equal to that of the graduation line image, graduation line signals of a triangle wave are generated successively from the photoelectric detector.

One of us previously analyzed in detail Eppenstein's principle [2]. Under the condition, the optical detecting system for graduation lines and the interferometer are connected; the distance between the graduation line O to be calibrated and the corner point of the corner cube MC is set to equal the focal length of the objective L4. Therefore, it is possible to calibrate line standards up to 2 m with the carriage having a traveling distance of 2 m.

The line standard is aligned by finely adjusting its position in the vertical or the horizontal direction relative to the optical axis, while observing the graduation line image through the microscope.

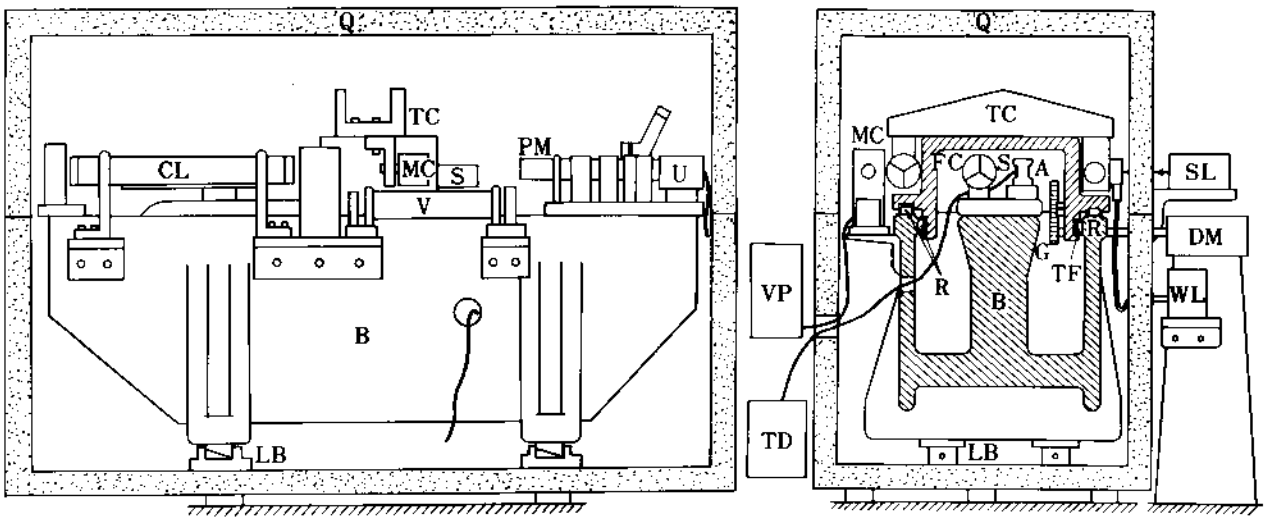

Fig. 2. Mechanical scheme: B, base; TC, carriage; LB, leveling block; CL, collimator; PM, photo-electric microscope; VP, vacuum pump; TD, thermometer; R, roller bearing; TF, teflon bearing; Q, environmental chamber

2.2. Mechanical System

Figure 2 shows schematically the mechanical system of this apparatus. A cast-iron bed, 290 cm long, 50 cm high, 40 cm wide, and weighing about 1000 kg, is supported on three leveling blocks LB. The overall system is placed in a double-walled chamber Q made of 8 cm thick insulating material inserted between two aluminium plates, and this is placed in a thermo-hygrostated room. Before measurement, fans are used to condition the chamber to a certain temperature near 20 °C. The laser light source SL, the illumination light source WL, the temperature measuring device TD, and the carriage drive motor DM are placed outside the chamber Q.

Rotation of the synchronous motor DM is transmitted to a pulley at one end of the bed by a multistage reduction gear mechanism G. The carriage is caused to travel by driving the endless stainless-steel tape T tensioned between the said pulley and another pulley at the other end of the bed. The carriage TC, weighing about 13 kg, is supported by four ball-and-roller bearings R. It is spring-loaded with an elastic force of about 10 N in contact with the side guide face of the bed by two ball-and-roller bearings R and two sliding teflon bearings TF. Traveling speed of the carriage can be changed optionally in eight stages between 10 and 300 mm/min.

Possible distortions of the bed, arising from motion of the carriage, could certainly lead to errors which would not be detected by the scatter of repeated measurements. This is because the supporting rest for line standard and the fixed corner cube are mounted firmly on the same block in the bed, and their relative displacements are eliminated.

2.3. Electronic System

Shown in Fig. 3 is the electronic system for forming a gate pulse from a graduation line signal to count interference fringes. The signal is initially amplified and then differentiated after eliminating noise by a low-pass filter. The electric-differential signal is amplified to form a steep pulse which indicates the zero crossing position; this pulse becomes the gate pulse.

There is a 90°-phase difference between two interference fringe signals from the photomultiplier tubes. After shaping both signals, eight pulses are generated each time the moving corner cube moves by a distance

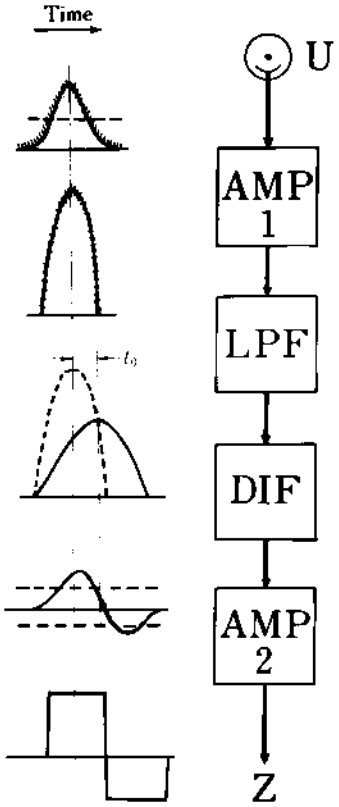

Fig. 3. Electronic waveforming process: U, photomultiplier tube; AMP1, AMP2, amplifiers; LPF, filter; DIF, differentiator; Z, zero-crossing detector

corresponding to half a wavelength. This implies that the fringe resolving power of this apparatus is $\lambda/16$.

A deviation of each line interval of the line standard to be calibrated from the nominal length counted is displayed on a display tube, and concurrently inputted into the memory of a computer through a telephone line. In addition, parameters such as temperature of the line standard and refractive index of the air during measurement are inputted. Finally, the result of the measurement is printed out after adequate corrections are made.

3. Positioning Accuracy

In this section are examined the noise of a graduation line signal and defocusing in image formation, each of which unfavorably influences accuracy of positioning the graduation lines.

3.1. Error due to Noise of Graduation Line Signal

The noise of a graduation line signal causes increased deviation of the zero crossing position in its electric processing and also lower positioning accuracy. Therefore, the graduation line signal must pass through a low-pass filter (RC filter) to improve the signal-to-noise ratio. This filter, however, causes a time delay (t_0) of the signal peak, which increases with the time constant RC (s) of the filter. If speed fluctuation ΔV of the carriage occurs here, it results in a measurement error $RC\Delta V$ [8]. Therefore, it is necessary to reduce speed fluctuation of the carriage to improve positioning accuracy.

The carriage is pulled by a steel tape, both forming vibration system. The characteristic frequency of the vibration system can be described simply by $\{(l_1^{-1} + l_2^{-1})\, AE/M\}\ 1/2/2\pi$, where A is cross-sectional area of the tape, E is elastic modulus of the tape, M is mass of the carriage, and l_1 and l_2 are lengths of tapes on both sides of the carriage. In the present apparatus, therefore, the characteristic frequency amounts to about 11 Hz with $A = 0.17\ \text{mm}^2$, $E = 2.0 \times 10^5\ \text{N/mm}^2$, $l_1 = l_2 = 1.4$ m and $M = 13$ kg. If ball-and-roller bearings only are used in the translation mechanism for the carriage, no element for suppressing vibration exists. In this instance, the carriage travels with speed fluctuation corresponding to a frequency of more than 10 Hz, as shown in Fig. 4 (A).

This speed fluctuation can be reduced by using teflon sliding bearings. Teflon resin is a material whose coefficient of friction is low at a sliding speed of approximately 100 mm/min and proportional to sliding speed [12]. Therefore, this material is useful for reducing vibration. Shown in Fig. 4 (B) are the experimental results of speed fluctuations in an arrangement in which two of the four ball-and-roller bearings in the translation mechanism for the carriage were replaced by teflon sliding bearings. This figure reveals that speed fluctuation of more than 10 Hz is reduced to about 10%.

In the improved arrangement, each graduation line interval in a line standard made of metal was measured fifteen times with various time constants RC of the low pass filter at a carriage speed of 100 mm/min. The line standard used has a H-cross section, and each of its graduation lines has a V-groove about 4 μm wide. The standard deviations of measured values are shown in Fig. 5. The figure shows that at that speed, the standard deviation becomes smaller with increasing the time constant RC until it reaches 1.3 ms, and gradually becomes larger with RC, when this exceeds the said value under the influence of carriage speed fluctuation. With the optimum time constant, the error of positioning is held to within 0.04 μm. This also occurs with a carriage speed of 30 mm/min; the optimum time constant, however, is larger at this carriage speed.

3.2. Error due to Defocusing

Image formation of graduation lines out of the focal point (i.e. defocusing) causes not only reduced contrast of the images but also distortion of those forms, resulting in lowered accuracy of measurement in connection with electrical characteristics of the wave processing system for graduation line signals [13].

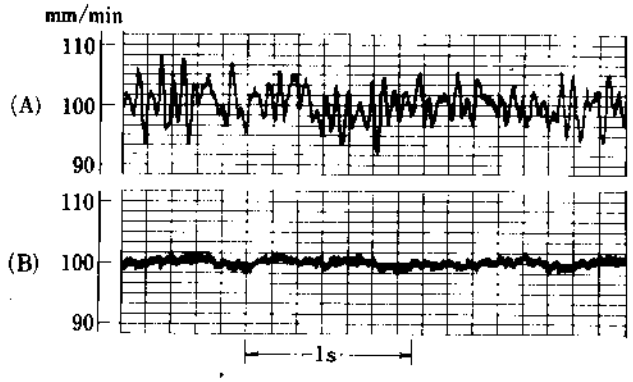

Fig. 4. Speed fluctuations of the carriage: (A), without teflon bearings; (B), with teflon bearings

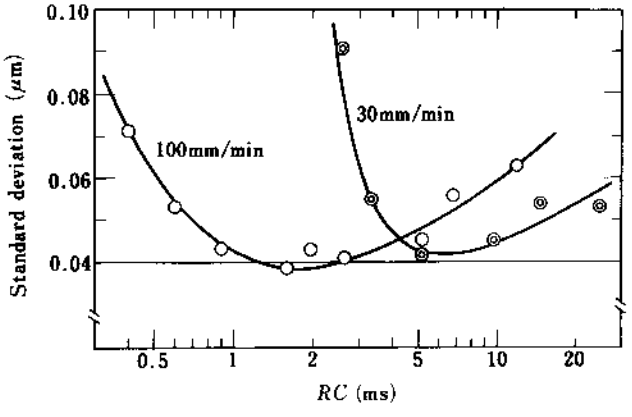

Fig. 5. Standard deviations of measured values as a function of time constant RC

To examine the influences of this defocusing, a line standard was displaced from its normal position in the direction of the optical axis in the optical image formation system, and the amount of this displacement was measured with an electric micrometer. The magnitude of defocusing is determined from the measured amount of displacement. Figure 6 shows standard deviations in measuring a line standard as a function of the magnitude of defocusing. The line standard used is glass with metal-evaporated graduation lines about 4 μm wide with intervals of 1 mm. Measurement was performed fifteen times for forward travel (F) and backward travel (R) of the carriage, each at a speed of 100 mm/min. It is evident from the figure that the standard deviations of measured values in the two instances enlarge as the magnitude of defocusing increases. This occurs because the tops of graduation line signals become gentle, and positioning worsens as contrast of the line images is lowered by defocusing. Moreover, Figure 6 shows a marked difference in standard deviation between results derived during alternate directions of carriage travel. The average value of measurements in one direction changed somewhat with defocusing, although the average value in both directions did not change very much within 0.04 μm. It is probable that the position upon forming a gate pulse in a graduation line signal is systematically transformed into the front part, deviated from the signal top with defocusing by finely different forms of individual lines and electric characteristics, particularly the frequency characteristic of the signal processing system. If focusing is conducted carefully, or if the results of measurement in both travel directions are averaged, the influence of possible defocusing is practically negligible, because the objective in the image formation system has a relatively small numerical aperture of 0.12.

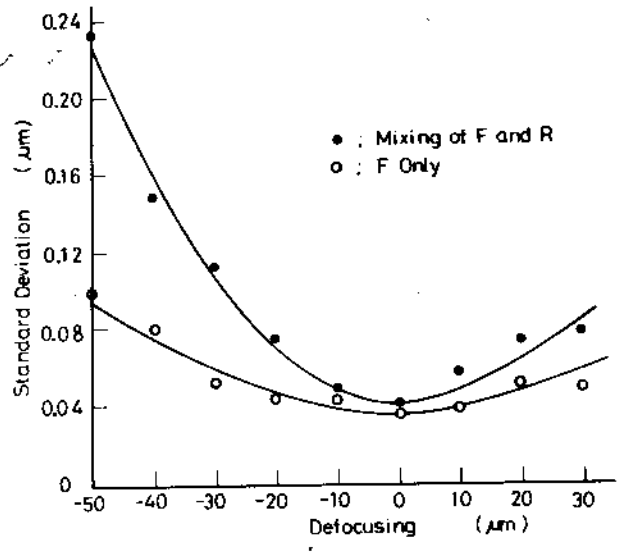

Fig. 6. Standard deviations of measured values as a function of defocusing

4. Evaluation of Accuracy

4.1. Adjustment of Optical System

Eppenstein's condition described in the latter part of Section 2.1 is satisfied by fine adjustment of the objective L4 and the corner cube MC in the optical system attached to a massive bracket secured on the carriage. The carriage travels with pitching and yawing of angles of less than ± 5 seconds. In the present apparatus, the optical system is so adjusted that the error of measurement due to deflection is up to several nm.

The travel direction of the carriage and the direction in which the light beam enters the corner cube MC are adjusted to be parallel to each other within 2×10^{-4} radian. Therefore, the error of measurement due to possible nonparallelism is up to 2×10^{-8}.

4.2. Reproducibility of Laser Wavelength

The laser used is a Lamb-dip stabilized He-Ne laser (Spectra Physics model 119). The wavelength of this laser in a vacuum and its stability were determined from measuring the beat frequency using an iodine molecule frequency stabilized laser [13, 14]. The measurements show that the wavelength of the Lamb-dip stabilized laser in a vacuum is 632.99143_4 nm and its stability is 1×10^{-8}, nearly corresponding to the modulated amplitude of the laser, while its reproducibility is better than 2×10^{-8}.

4.3. Measurement of Refractive Index of Air

The refractive index of air is measured by a Fizeau-type interferometer. The vacuum cell has a cross-sectional area of 15×25 mm^2 and is about 500 mm long (see Fig. 1). In consideration of residual gas in the vacuum cell, the dimensional error of the cell, and the error of reading fringes, measurement accuracy is evaluated to be up to 4×10^{-8}. In addition, the integer part of the order of interference is determined by measuring the atmospheric pressure, the water vapor pressure, and the air temperature, using a dispersion formula for the refractive index of air [16, 17].

4.4. Control and Measurement of Temperature

Room temperature and the water vapor pressure can be stably controlled within ±0.2 °C and ±130 Pa, respectively. The gradient of temperature on the line standard is within 0.002 °C, because the entire interferometer is placed in the insulated chamber. Temperature measurement is achieved by using a copper-constantan thermocouple-thermometer and a quartz thermometer. The temperature (near 20 °C) of liquid paraffin in the Dewer-cell is first measured as a reference point of temperature by the quartz thermometer. Then, the thermocouple thermometer is used to measure small temperature differences between the reference point and the line standard, and between the point and the air. Electromo-

tive force in the thermocouple is measured by the displacement method, using a dc reflecting galvanometer of high sensitivity. The quartz thermometer used was calibrated with an accuracy of 0.001 °C by means of platinum resistance thermometer. By employing this system, an accuracy of 0.004 °C is guaranteed in measuring temperature of the line standard.

5. Results of Measurement and Discussion

5.1. Results of Measurement

To investigate the overall accuracy under different measurement conditions, a 1 m long line standard (Hilger Watts 69/71), having graduation lines of V-cross sections about 4 μm wide, was caibrated once a day for four days. One measurement implies two traveling motions of the carriage forward and backward at a speed of 100 mm/min. The first two measurements were performed in the normal position of the line standard, the last two in its reversed position. Table 1 shows the partial results of such measurements. There are more or less differences between standard deviation in individual graduation lines. This is due to their different qualities. In the measurements of graduation lines in the range of 1 to 5 mm, the standard deviation is slightly larger than that described in Section 3. This is believed to be caused by an error of positioning in the forward and backward directions of the carriage because the graduation line signals are not perfectly symmetrical, and by a focusing error in the image formation system in reversal of the line standard to be calibrated. This standard deviation is practically uniform in the measurements of the graduation line intervals up to nearly 500 mm, but becomes about 0.02 μm larger in the graduation line intervals near 1000 mm. It is likely that this results from measurement errors and variations of the temperature of the line standard and the refractive index of air. The amount of scatter also depends on reproducibility of the laser wavelength.

Table 1. Experimental results

Interval (mm)	Mean Scale Correction (μm)	Standard Deviation (μm)
0– 1	+0.12	0.07
0– 2	−0.11	0.03
0– 3	+0.38	0.06
0– 499	−1.67	0.05
0– 500	−1.48	0.06
0– 501	−1.70	0.06
0– 998	−0.23	0.09
0– 999	−0.50	0.08
0–1000	−0.19	0.07
500– 998	+1.24	0.07
500– 999	+0.99	0.05
500–1000	+1.30	0.06

5.2. Discussion

The accuracy of positioning of graduation lines in automatic calibration of a line standard is generally low compared with that obtained in "static calibration". Particularly in the case of graduation lines of poor quality, this tendency is distinct.

In our apparatus designed on Eppenstein's principle, however, an objective having a numerical aperture slightly smaller than that of an ordinary photoelectric microscope and a relay-lens system for image formation are used in combination with a low-pass filter for improving the signal-to-noise ratio of graduation line signals to raise positioning accuracy. In addition, the use of teflon sliding bearings enables the necessary reduction of carriage speed fluctuation. Experiments have shown that the influence of defocusing in the optical image formation system can be suppressed considerably by measurement in two traveling directions of the carriage.

The standard deviation in measurements of a 1 m long line standard is about 0.08 μm in our apparatus. The cosine error due to deflection of the laser beam from the traveling direction of the carriage, which causes a substantial systematic error of measurement in the interferometer, is held to within 0.02 μm per 1 m. In considering parameters such as temperature of the line standard and the refractive index of air, absolute accuracy is evaluated to be 0.1 μm per 1 m provided each graduation line to be measured is of good quality.

6. Conclusion

An automatic laser interferometer for calibrating line standards up to 2 m was described as to its principle of measurement, structure, and function. The accuracy of this apparatus was evaluated experimentally by measuring a 1 m line standard. The results are as follows:

(1) Error of measurement due to nonparallelism of the light beam to the carriage and deviation from Eppenstein's condition was held up to 0.02 μm by adjustment of the optical system.

(2) In a range of carriage speed between 10 and 300 mm/min, the standard deviation in positioning of graduation lines was within 0.04 μm, and standard deviation in measurement of a 1 m line interval was 0.08 μm.

(3) Considering the accuracies of measurements of the refractive index of air with the Fizeau-type interferometer and the temperature of the line standard with a thermometer, overall accuracy is evaluated to be better than 0.1 μm per 1 m.

References

1. K.M. Baird: Rev. Sci. Instrum. **32**, 549 (1961)
2. Y. Sakurai, S. Takahashi, K. Ota: Bull. Nat. Res. Lab. Metrology **5**, 1 (1962)
3. P. Carré: Metrologia 2, 13 (1966)
4. K.E. Gilliland, H.D. Cook, K.D. Mielenz, R.B. Stephens: Metrologia 2, 95 (1966)
5. P.E. Ciddor, C.F. Bruce: Metrologia 3, 109 (1967)

6. Chr. Hoffrogge, H. Rummert: Metrologia **4**, 68 (1968)
7. Y. Doi, K. Shimizu, T. Tsuboi, T. Kohno: Appl. Opt. **3**, 817 (1964)
8. Y. Sakurai: Ann. C. I. R. P. **16**, 145 (1968)
9. S. Seino, Y. Sakurai, Y. Abe: J. Japan Soc. Precision Engineering **41**, 44 (1975) [in Japanese]
10. H. Matsumoto, Y. Sakurai, S. Seino: J. Japan Soc. Precision Engineering **44**, 226 (1978) [in Japanese]
11. E.R. Peck: J. Opt. Soc. Am. **52**, 253 (1962)
12. K. Matsubara: J. Mechanical Laboratory **10**, 27 (1956) [in Japanese]
13. H. Matsumoto: J. Japan Soc. Precision Engineering **45**, 1497 (1979) [in Japanese]
14. N. Ito, K. Tanaka: Metrologia **14**, 47 (1978)
15. S. Iwasaki, T. Sakurai: Oyo Buturi **49**, 870 (1980) [in Japanese]
16. T. Masui: Rev. Opt. **36**, 281 (1957)
17. B. Edlén: Metrologia **2**, 71 (1966)